Optimisation of horizontal annular finned tube under natural convection heat transfer

Hossain Nemati[1*], Mohammad Moghimi Ardekani[2], Ali Cemal Benim[3], Josua Meyer[4] 1

Department of Mechanics, Marvdasht Branch, Islamic Azad University, Marvdasht, Iran [2]

Department of Engineering, Staffordshire University, Stoke-on-Trent, UK

[3]Center of Flow Simulation (CFS), Department of Mechanical and Process Engineering, Düsseldorf University of Applied Sciences, Düsseldorf, Germany

[4]Clean Energy Research Group (CERG), Department of Mechanical and Aeronautical Engineering, University of Pretoria, Pretoria, South

[*] Corresponding author
Email: H.nemati@miau.ac.ir
Tel.: +987143112201

Abstract:

Free convection heat transfer over annular finned tubes was studied numerically for more than sixty different cases and verified against two experimental works. In addition, the effect of fin spacing on heat transfer was investigated. As a result, a correlation was proposed to estimate *Nusselt* number as a function of *Rayleigh* number. Moreover, it was shown that there was an optimum fin spacing for which the total heat transfer was maximised. Based on the proposed equation, an expression for optimum fin spacing was derived, which proved that the optimum *Nusselt* number was 0.9035. The presented equation for optimum fin spacing was a general equation in so far that it could also be used to find the optimum spacing between a series of circular disks by letting the tube diameter in the equation be zero. Moreover, a good agreement was observed between the derived equation for optimum fin spacing and the results of the scale analysis method.

Introduction

Natural convection heat transfer is an efficient mode of heat transfer that has been studied for different objects with different shapes [1-8]. In many cases, natural convection is not strong enough [9, 10]. Therefore, using extended surfaces in these cases to enhance heat transfer is mandatory. Many researchers have studied natural convection from extended surfaces, numerically or experimentally [11-13]. However, the study of an extended surface under natural convection heat transfer goes back to the experimental works of Elenbaas [14] on vertical plate-fin heat sinks. Edwards and Chaddock [15] studied heat transfer from horizontal finned tubes. Several experimental works can be found on heat transfer from a finned tube [16-28]. Since using an extended surface is the most viable and practical way to

enhance heat transfer, geometry optimisation is demanding, especially in cases where weight plays an important role.

The history of the optimisation of an extended surface is as old as natural convection study [29-32]. Again, Elenbaas [14] was the first to report the existence of an optimum fin spacing for a plate-fin heat sink. Bar-Cohen [33] derived the optimum fin spacing for a plate-fin heat sink. He proved that the *Nusselt* number value at that optimum fin spacing was equal to 1.25. Other techniques such as computational fluid dynamics (CFD) or entropy generation minimisation (EGM) were later used to improve the design of plate-fin heat sinks [34, 35].

In spite of numerous studies in optimising plate-fin heat sinks [19, 29, 31, 36, 37], a very limited number of studies focused on optimising the fin spacing for annular fins under natural convection heat transfer. Edwards and Chaddock [15] did a series of experiments on copper fins with diameter ratio $D/d = 5.17$, and proposed a correlation for Nusselt number (*Nu)*. They then differentiated their equation with respect to fin spacing and solved for the zero to find optimum fin spacing. The result was $Ra_s = 37$. However, this optimum *Rayleigh* number was only for $D/d = 5.17$ and Ra_s did not reflect the effect of tube diameter.

Littlefield and Cox [30] used the Tsubouchi and Masuda correlation [17] for *Nu* to optimise an annular fin considering fin efficiency. However, their work did not lead to an explicit correlation. Yildiz and Yüncü [38] used the scale analysis method to find the general form of the equation for optimum fin spacing. However, they did not have enough experimental data points to justify their finding (it was discussed in “Discussion” part in detail).

Recently, Wong and Lee [12] numerically simulated a series of aluminium and stainless steel horizontal annular fins. They showed that their results for optimum fin spacing were closer to Ref. [15] in comparison with Ref. [38]. Moreover, they correctly affirmed that none of these equations accounted for the effect of tube diameter, d.

To the best of the authors' knowledge, there is no explicit result (similar to that for plate-fin heat sink) to clarify the optimum R*ayleigh* number and its corresponding *Nusselt* number. The authors believe that a lack of extensive data points is the main reason why a precise expression for optimum fin spacing for an annular fin has not been presented. In this regard, the only wide-ranging experimental work was conducted by Tsubouchi and Masuda [17]. However, their proposed correlation is too complex to be used for deriving optimum fin spacing (see [30]).

In the present study, more than sixty different cases were numerically simulated. Unlike experimental methods, CFD provides a great facility to investigate different geometries. Numerical results were used to propose a functional relationship between the *Nusselt* and *Rayleigh* numbers. The proposed correlation was verified by two experimental works.

The optimum fin spacing was derived based on the proposed correlation. It was found that the optimum *Nu* for the optimum fin spacing was equal to 0.9035. The compatibility of the derived expression for the optimum fin spacing with the prediction of scale analysis method was presented. Finally, it was shown that the derived expression for optimum fin spacing could be generalised to cover the case of circular disks. It means that the optimum spacing between a series of circular disks can also be calculated using the presented expression by only setting the tube diameter to zero.

Numerical method and assumptions

The geometry of an annular fin with a diameter of D is shown in Fig. 1. Dashed lines indicate the symmetry boundaries at which the normal gradients of the variables as well as the normal velocity component are zero as boundary conditions. The exterior surface enclosing the solution domain (which has the diameter 5D in Fig. 1) is defined as pressure boundary with $P = P_{\infty}$, . In the case of inflow, the temperature of the fluid was set to be equal to the ambient temperature, i.e. $T = T_{\infty}$. At solid walls, the no-slip condition applied, i.e. u=v=w=0. The heat conduction in the tube and fin walls was coupled with the fluid domain, i.e. the conjugate heat transfer was considered. At the fluid-solid boundary interfaces, temperature and heat flux continuity applied:

$$k_s \left.\frac{\partial T}{\partial N}\right|_{\text{Solid}} = k \left.\frac{\partial T}{\partial N}\right|_{\text{Fluid}}, \; T_{\text{Solid}} = T_{\text{Fluid}} \tag{1}$$

At the inner-tube wall, the temperature was prescribed as boundary condition, i.e. $T = T_{\text{w}}$.

To reduce the tube wall resistance, a small value (1 mm) was assumed as the tube thickness (tube thickness was not shown in figures).

The three-dimensional governing equations with the assumption of steady-state laminar fluid flow are presented as follows:

Continuity:

$$\frac{\partial}{\partial x}(\rho u)+\frac{\partial}{\partial y}(\rho v)+\frac{\partial}{\partial z}(\rho w)=0 \tag{2}$$

Momentum equation:

$$\rho\left(u\frac{\partial u}{\partial x}+v\frac{\partial u}{\partial y}+w\frac{\partial u}{\partial z}\right)=-\frac{\partial P}{\partial x}+\mu\nabla^2 u \tag{3}$$

$$\rho\left(u\frac{\partial v}{\partial x}+v\frac{\partial v}{\partial y}+w\frac{\partial v}{\partial z}\right)=-\frac{\partial P}{\partial y}+\mu\nabla^2 v-\rho g \tag{4}$$

$$\rho\left(u\frac{\partial w}{\partial x}+v\frac{\partial w}{\partial y}+w\frac{\partial w}{\partial z}\right)=-\frac{\partial P}{\partial z}+\mu\nabla^2 w \tag{5}$$

Energy equation in the fluid zone:

$$\rho c_p\left(u\frac{\partial T}{\partial x}+v\frac{\partial T}{\partial y}+w\frac{\partial T}{\partial z}\right)=k\nabla^2 T \tag{6}$$

Energy equation in the solid zone:

$$0=\nabla^2 T \tag{7}$$

Fin material was aluminium and k_s =237 W/mK. Coolant fluid was assumed to be dry air and ideal gas:

$$P=\rho RT \tag{8}$$

With the exception of air density, all other thermophysical properties were assumed constant and evaluated at the film temperature, T_{film} :

$$T_{\text{film}}=\frac{T_w+T_\infty}{2} \tag{9}$$

The governing equations of the steady-state buoyancy-driven airflow were numerically solved using the CFX module of ANSYS 18.0, which uses an element-based finite volume method formulation along with a Rhie-Chow methodology [39] to treat the velocity-

pressure coupling. Moreover, a high-resolution scheme was used to discretise the advection terms. The RMS residual target was set to 10^{-4} and all other settings left unchanged. A structured, hexahedral, polar pattern mesh was used to discretise the domain (Fig. 2). In this arrangement, finer grids generated around the centre of the domain where temperature and velocity gradients were steeper and coarser ones generated in the far-field.

A grid independence study was conducted to ensure the numerical accuracy of the results. This resulted in a grid with greater than 1.6×10^6 numbers of elements. An overview of the results of the grid independence study is provided in Table 1. The geometry and the assumed temperature difference underlying the grid independence study are presented in Table 2.

The influence of the far-field boundary was also checked as presented in Table 3. The same geometry mentioned in Table 2 was used for the independence test. Based on Table 3, five times the fin diameter was selected as far-field. More solving details may be found in [40].

In this study, more than sixty different cases were modelled and simulated. Table 4 shows the ranges of parameters used in these simulations.

In these ranges, eight, four and five distinct values were selected for d, D and S respectively. The researchers tried to choose uniformly scattered data all over the domain. Finally, during the data reduction process, wherever it was found that the data resolution was not sufficient, some additional data points were considered.

Data validation

To verify the described CFD methodology, a two-step validation was proposed. As the first step, the discussed CFD method was implemented on a bare long tube (a long tube with no fin). This step was designed to validate the numerical simulation of the study in a special case (the natural convection over a horizontal long cylinder–no–fin condition).

Therefore, for a horizontal long cylinder, Ra_d is defined as [10]:

$$Ra_d = \frac{g\beta(T_w - T_\infty)d^3}{v\alpha} \tag{10}$$

and *Nu* based on cylinder diameter is [10]:

$$Nu_d = \frac{hd}{k} \tag{11}$$

Numerical results of this step are listed in Table 5 and compared with two well-known experimental correlations of Churchill and Chu [41] (Eq.(12)) and Morgan [42] with a maximum uncertainty of ±5% (Eq. (13)). The comparison shows good agreement between the numerical and experimental data and confirms the validity of the proposed CFD approach for the no-fin condition.

$$Nu_d = \left[0.6 + \frac{0.387 Ra_d^{\frac{1}{6}}}{\left[1 + (0.559/Pr)^{9/16}\right]^{8/27}}\right]^2 \qquad 10^{-5} < Ra_d < 10^{12} \tag{12}$$

$$Nu_d = 0.48 Ra_d^{0.25} \qquad 10^4 < Ra_d < 10^7 \tag{13}$$

In addition, to verifying the validity of the proposed numerical model for horizontal annular finned tube conditions, the second step of verification was proposed. In this step,

the experimental correlation for horizontal annular finned tube was compared with the presented numerical approach. In this regard, the results of eight random different cases with D/d =2.25 and S/d =0.185 to 1.0 were compared with the experimental correlation of Jones and Nwizu [43] given by Eq. (14). The comparison results are presented in Fig. 3.

$$Nu = 0.116\left(Ra\left(1+\frac{d}{D}\right)\right)^{0.53}\left[1-\exp\left(\frac{-155}{Ra\left(1+d/D\right)}\right)\right]^{0.26} \qquad 1 < Ra < 3\times10^{3} \tag{14}$$

where *Ra* and *Nu* are defined based on Eqs. (15) and (16). As displayed in Fig. 3, a good agreement between the results confirms the reliability of the proposed CFD approach for the horizontal annular finned tube cases. The mean absolute percentage error (MAPE) is 11.6%.

Data Reduction

All numerical results can be presented in the form of two dimensionless parameters, *Ra* and *Nu*.

For a horizontal annular finned tube, *Ra* is presented as [40]:

$$Ra = \frac{g\beta\left(T_w - T_\infty\right)S^3}{v\alpha}\left(\frac{S}{D+d}\right) \tag{15}$$

where all thermophysical properties are evaluated at mean temperature. *Nu* is based on fin spacing, *S*, is defined as [10]:

$$Nu = \frac{hS}{k} \tag{16}$$

In the above equation, *k* is the air thermal conductivity. The convective heat transfer coefficient, *h*, is calculated by [10]:

$$h = \frac{Q}{\left(\eta_f A_f + A_b\right)\left(T_w - T_\infty\right)} \tag{17}$$

A_f and A_b are the fin and bare tube heat transfer areas respectively. η_f is fin efficiency and can be estimated by [44]:

$$\eta_f = \left[\frac{\tanh\left(\psi m L_f\right)}{\psi m L_f}\right]^{\psi} \tag{18}$$

$$\psi = 1 + 0.179\ln\left(D/d\right) \tag{19}$$

$$m = \sqrt{\frac{2h}{k_s t_f}} \tag{20}$$

where $L_f = \frac{D-d}{2}$, is the fin height. In Eq. (17), the same heat transfer coefficient was assumed for both fin and bare tube.

The collection of all results is presented in Fig. 4. For these results, the following expression was correlated with R^2 =0.996 and the standard error was 4.9%.

$$Nu = \frac{0.5756 Ra}{6.264 + Ra^{0.7481}} \tag{21}$$

$1 < Ra \le 1.9 \times 10^4$; $1.1 < D/d \le 7$; $0.0268 \le S/d < 1$

Fin spacing optimisation

Fin spacing effect

Fig. 5 shows heat transfer rate from one metre of a finned tube at the various numbers of fins per metre of the tube for temperature differences 80K and 40K. The temperature

difference is defined as the difference between tube and ambient temperature. By increasing the number of fins, the heat transfer area was augmented. Therefore, it was expected that the total heat transfer increased monotonically. However, as illustrated in Fig. 5, there was a specific fin number in which the heat flux was maximised (see the circles in Fig. 5). As is clear, this optimum value is a function of temperature difference between the tube wall and air.

To understand the reason for the existence of optimum fin spacing, the temperature contours and velocity profiles were studied for this fin geometry at the temperature difference of 40K.

Fig. 6 shows temperature contours between two adjacent fins with different fin spacings. For a fin number equal to 276 fins/m (S=3.22 mm), the temperature variation in the horizontal direction was vanishingly small, implying a weak buoyant force. By increasing the fin spacing from S=3.22 mm to S=8.07 mm (for 118 fins/m), a temperature difference can be observed between the central zone and the zone adjacent to the fin wall. At wider fin spacing (e.g. 39 fins/m), a central plume can be observed rising from the middle of the tube. The term “Central peak” in Fig. 6 indicates this rising plume. The fluid boundary layer developing on the fin walls became thin because of this rising plume. Therefore, it was expected that the heat transfer would also get boosted.

On the other hand, increasing the fin spacing reduced the total heat transfer area per unit length of the tube. This reduction in heat transfer area was compensated for by the increase in heat transfer rate at preliminary stages. At wider fin spacing, the synergistic effect of fin wall and tube boundary layers was reduced and total heat transfer was reduced

as well. As a result, there would be optimum fin spacing in which total heat transfer would be maximised.

To support the above explanation more quantitatively, the velocity profiles at two different horizontal lines (HL1 and HL2) are shown in Fig. 7. HL1 is in the midplane of fin length and HL2 is at the fin edge.

Fig. 7 confirms the above explanation about fin spacing effect. At very low fin spacing, the velocity was low and approximately the same in both HL1 and HL2. This shows that the buoyancy force relative to viscous drag was not strong enough to accelerate the air between fin walls. For the case 118 fins/m, although the velocity at HL1 was approximately the same as for the case 276 fins/m (around 0.04 m/s), the velocity at HL2 was three times as high as for the case 276 fins/m. For the case 39 fins/m, a secondary peak in velocity at the middle of the fin spacing can be observed. It was expected that this peak would be flattened at very wide fin spacing. For more information, see [45].

Optimum fin spacing

Starting with Eq. (15), for an isothermal annular fin:

$$Ra = \frac{g\beta\left(T_w - T_\infty\right)S^4}{\nu\alpha\left(D+d\right)} = XS^4 \tag{22}$$

where $X = \frac{g\beta\left(T_w - T_\infty\right)}{\nu\alpha\left(D+d\right)}$. Also, for a specified finned tube length, L:

$$S \approx L / n \tag{23}$$

where n is the number of fins.

$$A_f = \frac{\pi}{4}\left(D^2 - d^2\right).2.n = \frac{L}{S}\frac{\pi}{2}\left(D^2 - d^2\right) \tag{24}$$

and total heat transfer from fin surface is:

$$Q = A_f h\left(T_w - T_\infty\right) \tag{22}$$

Combining Eq. (16), Eq. (24) and Eq. (22) yields:

$$Q = \frac{L}{S}\frac{\pi}{2}\left(D^2 - d^2\right)Nu.\frac{k}{S}\left(T_w - T_\infty\right) \tag{26}$$

Using Eq. (21) and Eq. (22):

$$Q = \frac{L}{S}\frac{\pi}{2}\left(D^2 - d^2\right)\left[\frac{0.5756\,XS^4}{6.264+\left(XS^4\right)^{0.7481}}\right].\frac{k}{S}\left(T_w - T_\infty\right) \tag{27}$$

Rearranging Q to the following form:

$$Q = \frac{\pi}{2}kL\left(D^2 - d^2\right)\left(T_w - T_\infty\right)\underbrace{\left[\frac{0.5756XS^2}{6.264+\left(XS^4\right)^{0.7481}}\right]}_{B(S)} \tag{28}$$

Since the terms out of brackets are constant, maximising Q means maximising B(s), *i.e.*:

$$\frac{d}{ds}B(S) = 0 \rightarrow 6.264 + \left(XS^4\right)^{0.7481} - 1.4962\left(XS^4\right)^{0.7481} = 0$$

which yields $XS^4 = 29.648$ or according to Eq. (22):

$$Ra_{opt} = 29.648 \tag{29}$$

Therefore, the optimum fin spacing, S_{opt}, obeys the following equation:

$$S_{opt} = 2.333\left(\frac{v\alpha(D+d)}{g\beta(T_w - T_\infty)} \right)^{1/4} \quad (30)$$

or by substituting Eq. (29) into Eq.(21), the optimum *Nu* is:

$$Nu_{opt} = 0.9035 \quad (31)$$

Therefore, the optimum achievable *Nu* is 0.9035. It is interesting to note that this optimum *Nu* for a vertical plate-fin heat sink is equal to 1.25 [33].

Eq. (30) was derived for an isothermal fin for which the fin wall temperature was uniform. However, due to limited fin thermal conductivity, an amount of fin wall temperature variations may be observed for a real finned tube. The case of non-isothermal fin may be accommodated in Eq. (30), incorporating the fin efficiency as follows [24, 46]:

$$S_{opt} = 2.333\left(\frac{v\alpha\,(D+d)}{g\beta\,\eta_f\,(T_w - T_\infty)} \right)^{1/4} \quad (32)$$

in which η_f is fin efficiency.

Discussion

Comparison with numerical results

Fig. 8 shows two sets of numerical results. The fin efficiency of each point is also indicated in its vicinity. The cubic spline was fitted to each set. This cubic spline was used later to find the optimum value of fin spacing. Since these curves are based on numerical results, they simulate non-isothermal fin behaviour.

Optimum fin spacing was derived from Fig. 8 for each data set and compared with the results of Eq. (30) and Eq. (32) in Table 6. Good agreement can be observed, which shows

that Eq. (32) can predict well the optimum fin spacing for non-isothermal fins. The relative difference is 12%.

Comparison with the scale analysis method

Yildiz and Yüncu [38] tried to find the optimum fin spacing by scale analysis method. They argue that in the limiting case of a very small value of fin spacing, *S*, total heat transfer is proportional to the square of fin spacing. On the other hand, in the limiting case of fin spacing which is much greater than boundary layer thickness, total heat transfer is proportional to the inverse of fin spacing. Subsequently, they proposed Fig. 9 for the asymptotic plot of extreme limits. Equating the two asymptotes, they reached at the following expression for optimum fin spacing:

$$S_{opt} = 3.38\left(\frac{v\alpha(D)}{g\beta\eta(T_w - T_\infty)}\right)^{1/4} \tag{33}$$

By comparing Eq. (33) with Eq. (30), two differences can be observed. The first is that the coefficient of Eq. (33) is 45% larger than Eq. (30) (3.38 in comparison with 2.333) and the second is the presence of *d* in the nominator of Eq. (30). These two differences are discussed below:

- Difference in coefficients

Comparing with their experimental results, Yildiz and Yüncu [38] found that the coefficient of their proposed equation (Eq. (33)) was greater than the expected value. But they did not have enough experimental points to adjust the coefficient. However, they state the following:

"*It can be noted that, this scale analysis gives only an order-of-magnitude estimation. . . It would not be logical to expect the exact value of optimum fin spacing by this analysis.*"

- Presence of $D+d$ instead of D

Since they used scale analysis, they did not find the necessity of d in their analysis. However, they observed data scattering relative to their proposed correlation. Therefore, they argue as follows:

"*The scatter of the data may be due to approximate characteristic of the scale analysis and the uncertainty of the experiments.*"

With the exception of these two minor differences, it is interesting that their prediction based on the scale analysis method is well compatible with the present equation. This compatibility also shows that the *Nu* correlation (Eq. (21)) works well in the extreme limits. In other words, Eq. (21) itself is compatible with the scale analysis.

Comparison with the experimental results

Edwards and Chaddock [15] conducted a series of experiments to measure the free convection heat transfer from cylinders with uniform annular fins with three radius ratios (D/d = 1.94, 2.97 and 5.17) and three different fin and tube materials and six different fin spacings. The fins were thin, with a thickness of 0.508 mm, which is very close to the fin thickness of this study. They proposed a separate curve for each radius ratio and material. Then for copper fins with D/d = 5.17, they formulated heat transfer as a function of fin spacing and solved for the zero of derivative of that function to give $Ra_s = 37$, where

$$Ra_s = \frac{g\beta\left(T_w - T_\infty\right)S^4}{\nu\alpha\left(D\right)} \tag{34}$$

To compare it with the finding of this study, rearranging Eq. (29) and Eq. (22) as:

$$Ra_{opt} = \frac{g\beta(T_w - T_\infty)S^4}{v\alpha(D+d)} = \frac{1}{(1+d/D)} Ra_s = 29.648 \quad (35)$$

Replacing d/D=1/5.17 from the experiments of Edwards and Chaddock [15] yields:

$$Ra_s = (1+d/D)29.648 = 35.4 \quad (36)$$

35.4 is only 4% less than the reported value of 37. However, in contrast to Edwards and Chaddock's [15] prediction, the effect of D/d is included in the current study (Eq. (30)).

Comparison with parallel circular disks

One limiting case in this study was a finned tube with a very small diameter. As tube diameter approached zero, it resembled some vertical parallel circular disk (Fig. 10).

For rectangular fins, based on Abbas and Wang [47], the two adjacent developing boundary layers on the fin walls eventually meet at some point and form the fully developed flow. it is known that the heat transfer rate in the fully developed region, is considerably lower than the entrance region. For a large fin spacing, these two developing boundary layers may not meet each other before leaving the channel. So, the heat transfer rate is high but the total heat transfer area is low. On the other hand, for a narrow fin spacing, the boundary layers reach each other at the early entrance of the fin channel which results in a lower heat transfer rate, but the heat transfer area is high. So, it is expected to have a optimum fin spacing in which the total heat flux is maximized. In spite of more complexity for parallel circular disks, the same trend would be expected.

Tsubouchi and Masuda [17] proposed the following equation based on their experimental works on parallel vertical disks:

$$Nu = \frac{Ra_s}{6\pi}\left[1 - exp\left[-\left(\frac{25.3}{Ra_s}\right)^{3/4}\right]\right] \qquad 3 < Ra_s < 6\times10^3 \tag{37}$$

Substituting the above equation into Eq. (26) and using Eq. (22) yields:

$$Q = \frac{kLDS^2}{12}\frac{g\beta\left(T_w - T_\infty\right)^2}{\nu\alpha}\left[1 - \exp\left[-\left(\frac{25.3}{XS^4}\right)^{3/4}\right]\right] \tag{38}$$

in which $X = \frac{g\beta\left(T_w - T_\infty\right)}{\nu\alpha\left(D\right)}$.

Eq. (38) is presented for three different disk diameters in Fig. 11. This figure shows that there is an optimum fin spacing for heat transfer from a series of parallel disks also. However, this optimum fin spacing cannot be derived analytically from Eq. (38).

Eq. (30) is represented in Fig. 11 for *d*=0 by a solid thick line. As is clear even for the special case *d*=0, the proposed equation can present the optimum fin spacing for parallel circular disks.

Conclusions

In the present study, laminar natural convection heat transfer from annular finned tubes was studied numerically. A correlation was proposed to estimate *Nu* and was verified by some experimental works. The effect of fin spacing was also investigated. It was shown that there would be a specific fin spacing in which total heat transfer was maximised. For this optimum fin spacing, it was derived that $Ra_{opt} = 29.648$ and $Nu_{opt} = 0.9035$.

The presented equation for optimum fin spacing works even for parallel circular disks. It can be used to predict the optimum spacing between parallel disks if, in this equation, one puts the tube diameter equal to zero. Furthermore, it was shown that the present equation was compatible with the prediction of the scale analysis.

Nomenclature

A_b	bare tube surface area per unit length of the tube (m^2)
A_f	fin surface area per unit length of the tube (m^2)
c	fin pitch (m)
c_p	air isobaric specific heat capacity (J/kgK)
D	fin diameter (m)
d	tube outer diameter (m)
g	gravitational acceleration (m/s^2)
h	average convective heat transfer coefficient ($W/m^2.K$)
k	fluid thermal conductivity (W/m.K)
k_s	fin thermal conductivity (W/m.K)
L	tube length (m)
L_f	Fin height [$= \frac{D-d}{2}$] (m)
N	normal vector
Nu	*Nusselt* number based on fin spacing (Eq. (16))
Nu_d	*Nusselt* number based on cylinder diameter (Eq. (11))
Nu_{opt}	*Nusselt* number at optimum fin spacing
n	number of fins
P	pressure (Pa)
P_∞	ambient pressure (Pa)
Pr	Prandtl number

Q	total heat transfer (W)
q	heat flux (W/m^2)
R	air gas constant (J/kg.K)
R^2	coefficient of determination
Ra	*Rayleigh* number based on S, D, and d (Eq. (22))
Ra_d	*Rayleigh* number based on d (horizontal long cylinder) (Eq. (10))
Ra_{opt}	*Rayleigh* number at optimum fin spacing [=29.648]
Ra_s	*Rayleigh* number based on S and D (Eq. (34))
S	fin spacing (m)
S_{opt}	optimum fin spacing (m)
T	temperature (K)
T_{film}	film temperature [$=\frac{T_w + T_\infty}{2}$] (K)
T_w	fin surface temperature (K)
T_∞	ambient temperature (K)
u	x-component of the fluid velocity vector (m/s)
t_f	fin thickness (m)
v	y-component of the fluid velocity vector (m/s)
w	z-component of the fluid velocity vector (m/s)
x, y, z	Cartesian coordinates (m)

Greek symbols

α	air thermal diffusivity (m^2/s)
β	air thermal expansion coefficient (1/K)
ΔT	temperature difference [$=T_w - T_\infty$] (K)
η_f	fin efficiency
μ	air viscosity (Pa.s)
ν	air kinematic viscosity (m^2/s)
ρ	air density (kg/m^3)

Abbreviation

CFD	computational fluid dynamics
HL	horizontal line

References

[1] B. Li and C. Byon, "Experimental and numerical study on the heat sink with radial fins and a concentric ring subject to natural convection," *Appl. Therm. Eng.,* vol. 90, pp. 345-351, Nov. 2015. DOI: 10.1016/j.applthermaleng.2015.06.083.

[2] M. Lee, H. J. Kim, and D.K. Kim, "Nusselt number correlation for natural convection from vertical cylinders with triangular fins," *Appl. Therm. Eng.,* vol. 93, pp. 1238-1247, Jan. 2016. DOI: 10.1016/j.applthermaleng.2015.10.105.

[3] N. H. Saeid, "Natural convection in a square cavity with discrete heating at the bottom with different fin shapes," *Heat Transfer Eng.,* vol. 39, no. 2, pp. 154-161, Jan. 2018. DOI: 10.1080/01457632.2017.1288053.

[4] M. Ali, A. Nuhait, and R. Almuzaiqer, "The effect of square tube location in a vertical array of square tubes on natural convection heat transfer," *Heat Transfer Eng.,* vol. 39, no. 12, pp. 1036-1051, 2018. DOI: 10.1080/01457632.2017.1358485.

[5] S. Rath and S. K. Dash, "Numerical investigation of natural convection heat transfer from a stack of horizontal cylinders," *J. Heat Transfer,* vol. 141, no. 1, pp. 012501, Jan. 2019. DOI: 10.1115/1.4040954.

[6] K. G. B. M. Gowda, M. S. Rajagopal, and K. N. Seethramu, "Numerical Studies on Natural Convection in a Trapezoidal Enclosure With Discrete Heating," *Heat Transfer Eng.,* vol. 41, no. 6-7, pp. 595-606, 2020. DOI: 10.1080/01457632.2018.1546948.

[7] S. Durgam, S. P. Venkateshan, and T. Sundararajan, "Effect of thermal conductivity on cooling of square heat source array under natural convection in a vertical channel," *Heat Transfer Eng.,* vol. 41, no. 11, pp. 947-960, 2020. DOI: 10.1080/01457632.2019.1589986.

[8] H. Nemati, M. Moghimi, P. Sapin, and C. Markides, "Shape optimisation of air-cooled finned-tube heat exchangers," *Int. J. Therm. Sci.,* vol. 150, pp. 106233, Apr. 2020. DOI: 10.1016/j.ijthermalsci.2019.106233.

[9] A. Bejan, *Convection heat transfer*. New York, NY, USA, John Wiley & Sons, 2013.

[10] F. Kreith, R. M. Manglik, and M. S. Bohn, *Principles of heat transfer*. Cengage learning, 2012.

[11] M. Eslami and K. Jafarpur, "Laminar natural convection heat transfer from isothermal cylinders with active ends," *Heat Transfer Eng.,* vol. 32, no. 6, pp. 506-513, 2011. DOI: 10.1080/01457632.2010.506378.

[12] S.C. Wong and W.Y. Lee, "Numerical study on the natural convection from horizontal finned tubes with small and large fin temperature variations," *Int. J. Therm. Sci.,* vol. 138, pp. 116-123, Apr. 2019. DOI: 10.1016/j.ijthermalsci.2018.12.042.

[13] M. Ashouri, M. M. Zarei, and A. Hakkaki-Fard, "A Numerical Investigation on Natural Convection Heat Transfer in Annular-Finned Concentric Horizontal Annulus Using Nanofluids: A Parametric Study," *Heat Transfer Eng.,* vol. 42, no. 22, 2021 (in press). DOI: 10.1080/01457632.2020.1834215.

[14] W. Elenbaas, "Heat dissipation of parallel plates by free convection," *Physica,* vol. 9, no. 1, pp. 1-28, Jan. 1942. DOI: 10.1016/S0031-8914(42)90053-3.

[15] J. Edwards and J. Chaddock, "An experimental investigation of the radiation and free convection heat transfer from a cylindrical disk extended surface," *Trans. Am. Soc. Heat. Refrig. Air-Cond. Eng,* vol. 69, pp. 313-322, 1963.

[16] J. Knudsen and R. Pan, "Natural convection heat transfer from transverse finned tubes," *Chem. Eng. Progr,* vol. 59, no. 7, pp. 44-49, 1963.

[17] T. Tsubouchi and H. Masuda, "Natural convection heat transfer from horizontal cylinders with circular fins," *Proc. 6th Int. Heat Transfer Conf., Paper NC 1.10, Paris,* 1970.

[18] E. Sparrow and P. Bahrami, "Experiments on natural convection heat transfer on the fins of a finned horizontal tube," *Int. J. Heat Mass. Tran.,* vol. 23, no. 11, pp. 1555-1560, Nov. 1980. DOI: 10.1016/0017-9310(80)90159-3.

[19] C. Leung, S. Probert, and M. Shilston, "Heat exchanger: optimal separation for vertical rectangular fins protruding from a vertical rectangular base," *Appl. Energ.,* vol. 19, no. 2, pp. 77-85, 1985. DOI: 10.1016/0306-2619(85)90063-7.

[20] K. Jambunathan, R. Edwards, and B. Button, "Convective heat-transfer coefficients: The colour-change paint technique," *Appl. Energ.,* vol. 28, no. 2, pp. 137-152, 1987. DOI: 10.1016/0306-2619(87)90047-X.

[21] S. Naik, S. Probert, and C. Wood, "Natural-convection characteristics of a horizontally-based vertical rectangular fin-array in the presence of a shroud," *Appl. Energ.,* vol. 28, no. 4, pp. 295-319, 1987. DOI: 10.1016/0306-2619(87)90033-X.

[22] N. Kayansayan and R. Karabacak, "Natural convection heat transfer coefficients for a horizontal cylinder with vertically attached circular fins," *Heat Recov. Syst. CHP,* vol. 12, no. 6, pp. 457-468, Nov. 1992. DOI: 10.1016/0890-4332(92)90014-9.

[23] E. Hahne and D. Zhu, "Natural convection heat transfer on finned tubes in air," *Int. J. Heat Mass. Tran.,* vol. 37, pp. 59-63, Mar. 1994. DOI: 10.1016/0017-9310(94)90009-4.

[24] C. S. Wang, M. Yovanovich, and J. Culham, "Modeling natural convection from horizontal isothermal annular heat sinks," *J. Electron. Packaging,* vol. 121, no. 1, pp. 44-49, Mar. 1999. DOI: 10.1115/1.2792660.

[25] F. Harahap and D. Setio, "Correlations for heat dissipation and natural convection heat-transfer from horizontally-based, vertically-finned arrays," *Appl. Energ.,* vol. 69, no. 1, pp. 29-38, May 2001. DOI: 10.1016/S0306-2619(00)00073-8.

[26] A. Güvenç and H. Yüncü, "An experimental investigation on performance of fins on a horizontal base in free convection heat transfer," *Heat Mass Transfer,* vol. 37, no. 4-5, pp. 409-416, 2001. DOI: 10.1007/s002310000139.

[27] M. Yaghoubi and M. Mahdavi, "An investigation of natural convection heat transfer from a horizontal cooled finned tube," *Exp. Heat Transfer,* vol. 26, no. 4, pp. 343-359, 2013. DOI: 10.1080/08916152.2012.669809.

[28] D. Jang, S. J. Yook, and K. S. Lee, "Optimum design of a radial heat sink with a fin-height profile for high-power LED lighting applications," *Appl. Energ.,* vol. 116, pp. 260-268, Mar. 2014. DOI: 10.1016/j.apenergy.2013.11.063.

[29] C. D. Jones and L. F. Smith, "Optimum arrangement of rectangular fins on horizontal surfaces for free-convection heat transfer," *J. Heat Transfer,* vol. 92, no. 1, pp. 6-10, 1970. DOI: 10.1115/1.3449648.

[30] J. Littlefield and J. Cox, "Optimization of annular fins on a horizontal tube," *Wärme- und Stoffübertragung,* vol. 7, no. 2, pp. 87-93, Feb. 1974. DOI: 10.1007/BF01369516.

[31] B. Yazicioğlu and H. Yüncü, "Optimum fin spacing of rectangular fins on a vertical base in free convection heat transfer," *Heat Mass Transfer,* vol. 44, no. 1, pp. 11-21, 2007. DOI: 10.1007/s00231-007-0329-5.

[32] M. Söylemez, "Optimum length of finned pipe for waste heat recovery," *Energ. Convers. Manage.,* vol. 49, no. 1, pp. 96-100, Jan. 2008. DOI: 10.1016/j.enconman.2007.05.013.

[33] A. Bar-Cohen, "Fin thickness for an optimized natural convection array of rectangular fins," *J. Heat Transfer,* vol. 101, no. 3, pp. 564-566, Aug. 1979. DOI: 10.1115/1.3451032.

[34] T. Furukawa and W. J. Yang, "Reliability of heat sink optimization using entropy generation minimization," in *8th AIAA/ASME Joint Thermophysics and Heat Transfer Conference*, St. Louis, Missouri, USA, Jun 24-26, 2002. DOI: 10.2514/6.2002-3216.

[35] H. Nemati, "A general equation based on entropy generation minimization to optimize plate fin heat sink," *Eng. J-Canada.,* vol. 22, no. 1, pp. 159-174, 2018. DOI: 10.4186/ej.2018.22.1.159

[36] R. H. Yeh and M. Chang, "Optimum longitudinal convective fin arrays," *Int. Commun. Heat Mass,* vol. 22, no. 3, pp. 445-460, May-Jun. 1995. DOI: 10.1016/0735-1933(95)00029-X.

[37] G. Xu, Y. Cheng, and L. Luo, "Heat-transfer characteristics and design optimization for a small-sized plate-fin heat sink array," *J. Electron. Packaging,* vol. 129, no. 4, pp. 518-521, Dec. 2007. DOI: 10.1115/1.2804102.

[38] Ş. Yildiz and H. Yüncü, "An experimental investigation on performance of annular fins on a horizontal cylinder in free convection heat transfer," *Heat Mass Transfer,* vol. 40, no. 3-4, pp. 239-251, 2004. DOI: 10.1007/s00231-002-0404-x.

[39] C. Rhie and W. L. Chow, "Numerical study of the turbulent flow past an airfoil with trailing edge separation," *AIAA J.,* vol. 21, no. 11, pp. 1525-1532, 1983. DOI: 10.2514/3.8284.

[40] H. Nemati, M. Moradaghay, S. Shekoohi, M. Moghimi, and J. Meyer, "Natural convection heat transfer from horizontal annular finned tubes based on modified Rayleigh number," *Int. Commun. Heat Mass,* vol. 110, pp. 104370, Jan. 2020. DOI: 10.1016/j.icheatmasstransfer.2019.104370.

[41] S. W. Churchill and H. H. Chu, "Correlating equations for laminar and turbulent free convection from a horizontal cylinder," *Int. J. Heat Mass. Tran.,* vol. 18, no. 9, pp. 1049-1053, Sep. 1975. DOI: 10.1016/0017-9310(75)90222-7.

[42] V. T. Morgan, "The overall convective heat transfer from smooth circular cylinders," *Adv. Heat Transf.*, vol. 11, pp. 199-264, 1975. DOI: 10.1016/S0065-2717(08)70075-3.

[43] C. Jones and E.I. Nwizu "Optimum spacing of circular fins on horizontal tubes for natural convection heat transfer," *ASHRAE Symp. Bull. DV-69-3,* 11-15, 1969.

[44] H. Nemati and S. Samivand, "Simple correlation to evaluate efficiency of annular elliptical fin circumscribing circular tube," *Arab. J. Sci. Eng.,* vol. 39, no. 12, pp. 9181-9186, 2014. DOI: 10.1007/s13369-014-1474-z.

[45] H. Nemati and M. Moradaghay, "Parametric study of natural convection over horizontal annular finned tube," *J. Cent. South Univ.,* vol. 26, no. 8, pp. 2077-2087, 2019. DOI: 10.1007/s11771-019-4155-y.

[46] A. Bar-Cohen, M. Iyengar, and A. D. Kraus, "Design of optimum plate-fin natural convective heat sinks," *J. Electron. Packaging,* vol. 125, no. 2, pp. 208-216, Jun. 2003. DOI: 10.1115/1.1568361.

[47] A. Abbas and C. C. Wang, "Augmentation of natural convection heat sink via using displacement design," *Int. J. Heat Mass. Tran.,* vol. 154, pp. 119757, Jun. 2020. DOI: 10.1016/j.ijheatmasstransfer.2020.119757.

Table 1: Results of the grid independence study

Element Number (10^6)	0.05	0.13	0.30	0.82	0.95	1.6	2.29
q (W/m^2)	0.0732	0.0713	0.0709	0.0706	0.0704	0.0702	0.0701
Error	4.45%	1.63%	1.18%	0.64%	0.47%	0.17%	---

Table 2: Parameters used for the grid independence study

d (mm)	D (mm)	t_f (mm)	S (mm)	$T_w - T_\infty$ (K)
18.0	140	0.4	3.22	40

Table 3: Results of the study for domain size independence

Domain diameter	$2D$	$3D$	$4D$	$5D$	$8D$
q (W/m^2)	0.0767	0.0737	0.0716	0.0702	0.0702

Table 4: Range of simulated parameters

Dimension	d (mm)	D (mm)	S (mm)	t_f (mm)	$T_w - T_\infty$ (K)
Range	18-120	57.15-140	3.22-25.24	0.4	20, 40

Table 5: Long cylinder natural convection comparison

Ra_d	1.636 E4	5.043 E4	7.576 E4	1.473 E5	4.258 E5	1.242 E6	Max. Error
Nu_d [41]	4.91	6.69	7.21	8.98	11.98	16.15	12.0%
Nu_d [42]	5.43	7.19	7.96	9.40	12.26	16.02	3.5%
Nu_d	5.50	7.26	7.68	9.40	12.50	15.75	---

Table 6: Optimum fin spacing for non-isothermal fin, S_{opt} (mm)

$\Delta T = T_w - T_\infty$ (K)	Fig. 8	Eq. (30)	Eq. (32)
80	5.8	4.8	5.1
40	6.3	5.5	5.7

List of Figure Captions

Fig. 1. Sketch of the geometry and the solution domain

Fig. 2. Frontal view of the grid and its zoomed-in view

Fig. 3. Comparison of numerical CFD data points with experimental correlation of Jones and Nwizu [43].

Fig. 4. Comparison of numerical results and the proposed correlation (Eq. (21))

Fig. 5. Heat transfer rate from one metre of finned tube for various fin numbers per metre based on CFD results.

Fig. 6. Temperature contours between two adjacent fins plotted in the symmetry plane at z=0 (Fig. 1a), results mirrored around the symmetry plane at x=$c/2$ (Fig. 1b).
(note that the lower part of the domain is not shown in full)
d= 25.4 mm, D=57.15 mm, $\Delta T = 40$ °C

Fig. 7. Air velocity profiles between two fins.
d= 25.4 mm, D=57.15 mm, $\Delta T = 40$ °C

Fig. 8. Heat transfer rate from one metre of finned tube for various fin spacings based on CFD results.

Fig. 9. Asymptotic plot for extreme limits

Fig. 10. The limiting case, d=0 for annular fin (a) is similar to parallel circular disks (b)

Fig. 11. Variation of convection heat transfer rate for parallel circular disks with fin spacing at different disk diameters

(a) Side view of an infinite row of fins, dashed lines indicating symmetry planes at $x=0$ and $x=c/2$

(b) Frontal view, dashed lines indicating vertical symmetry plane

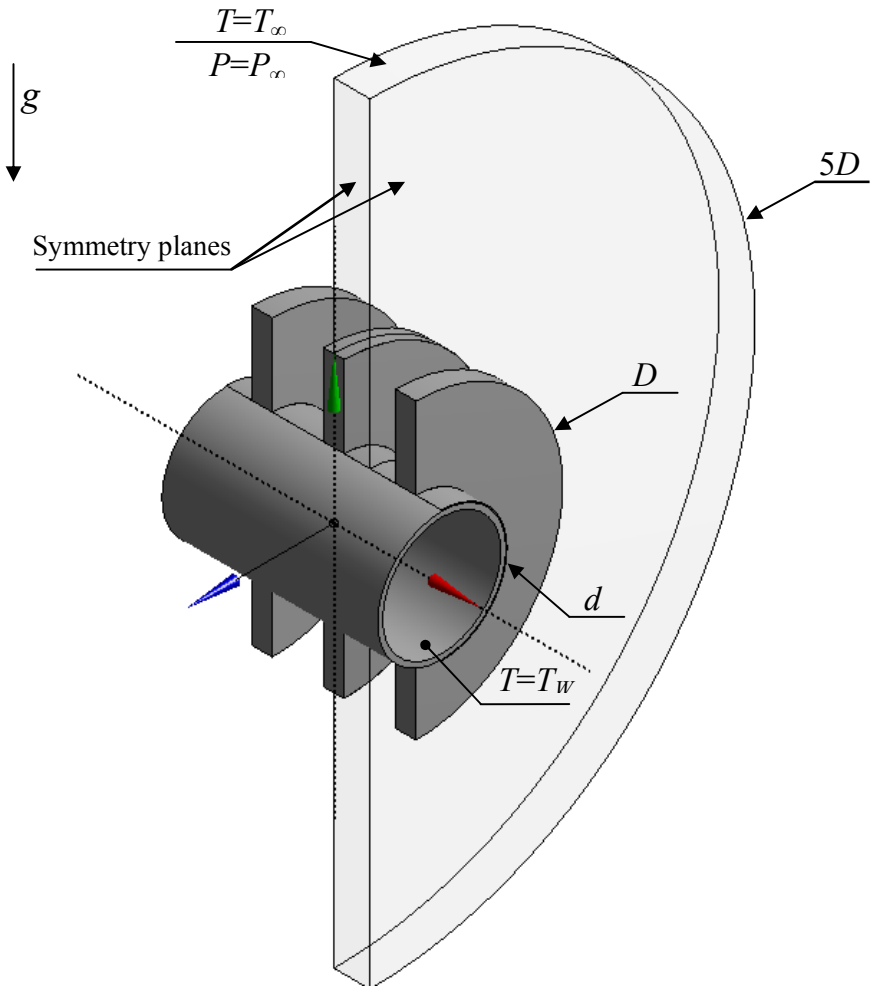

(c) 3D view of model

Fig. 1. Sketch of the geometry and the solution domain

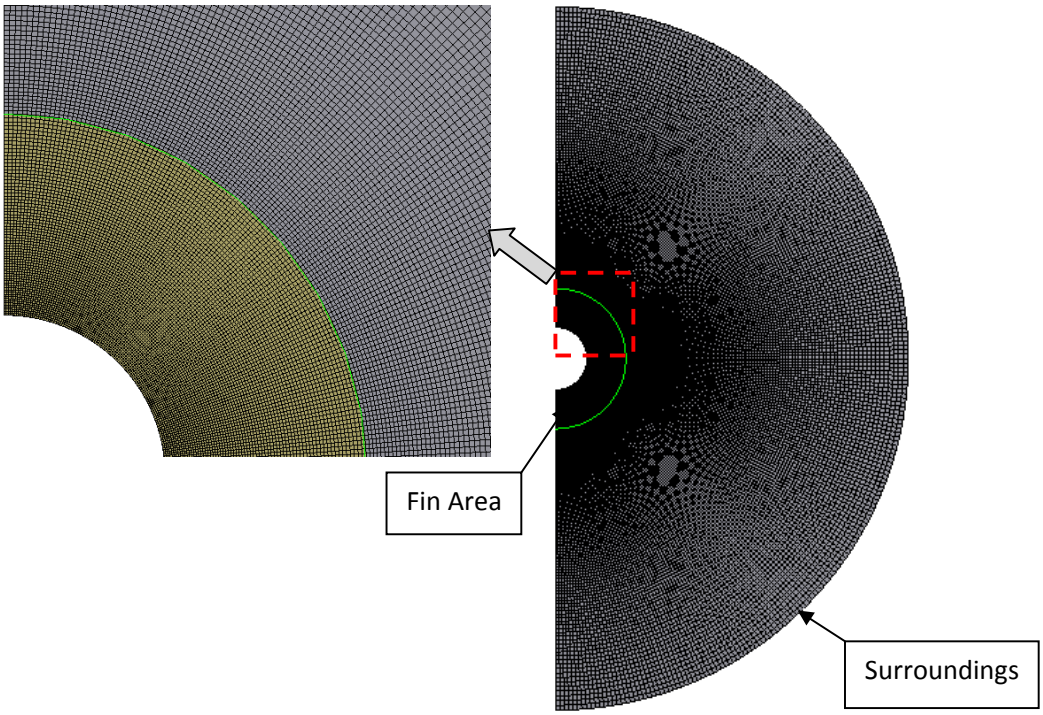

Fig. 2. Frontal view of the grid and its zoomed-in view

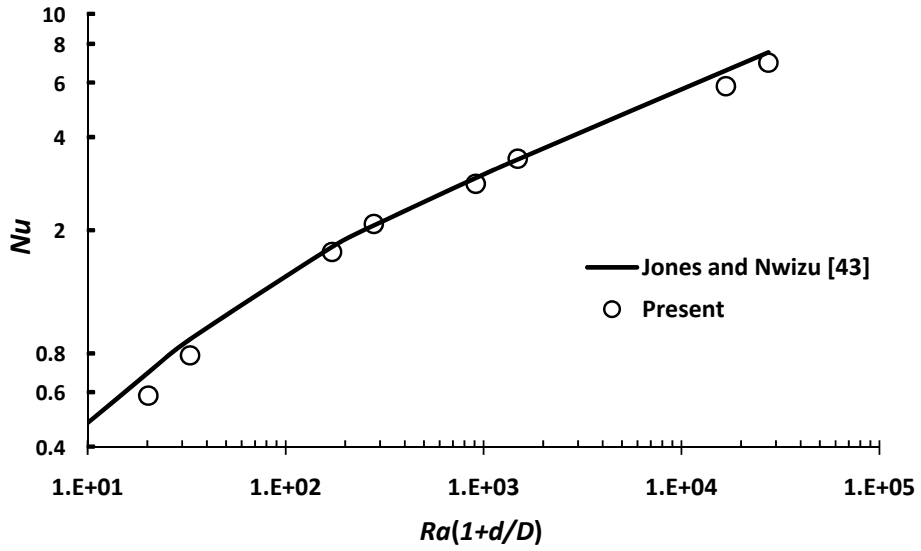

Fig. 3. Comparison of numerical CFD data points with experimental correlation of Jones and Nwizu [43].

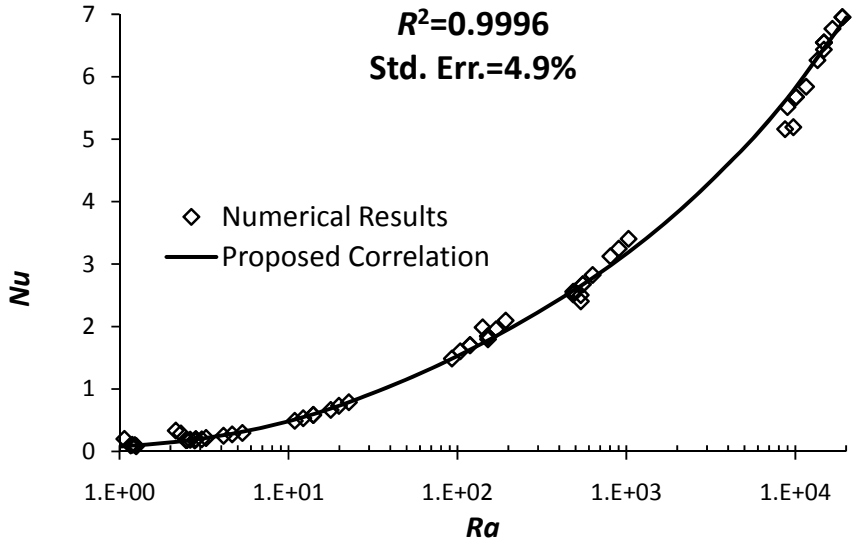

Fig. 4. Comparison of numerical results and the proposed correlation (Eq. (21))

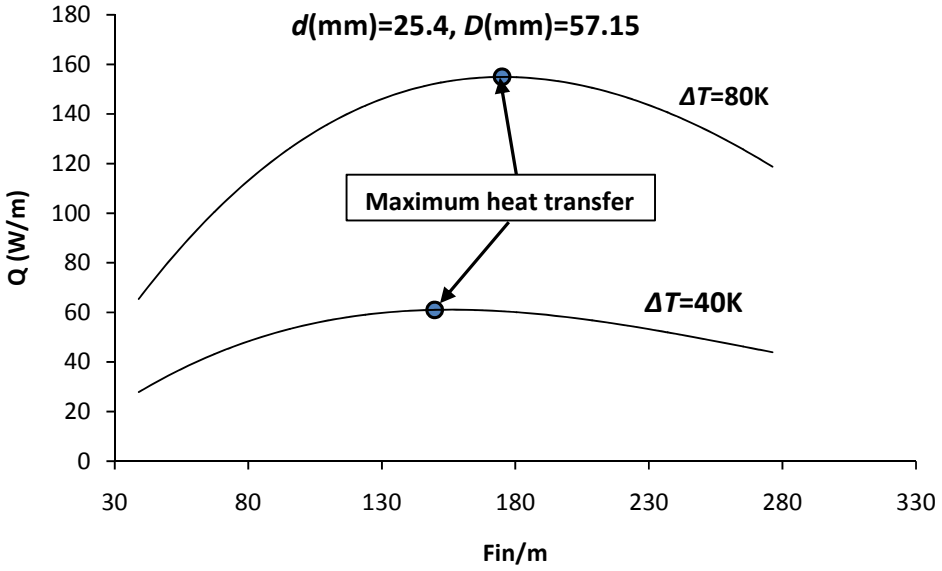

Fig. 5. Heat transfer rate from one metre of finned tube for various fin numbers per metre based on CFD results.

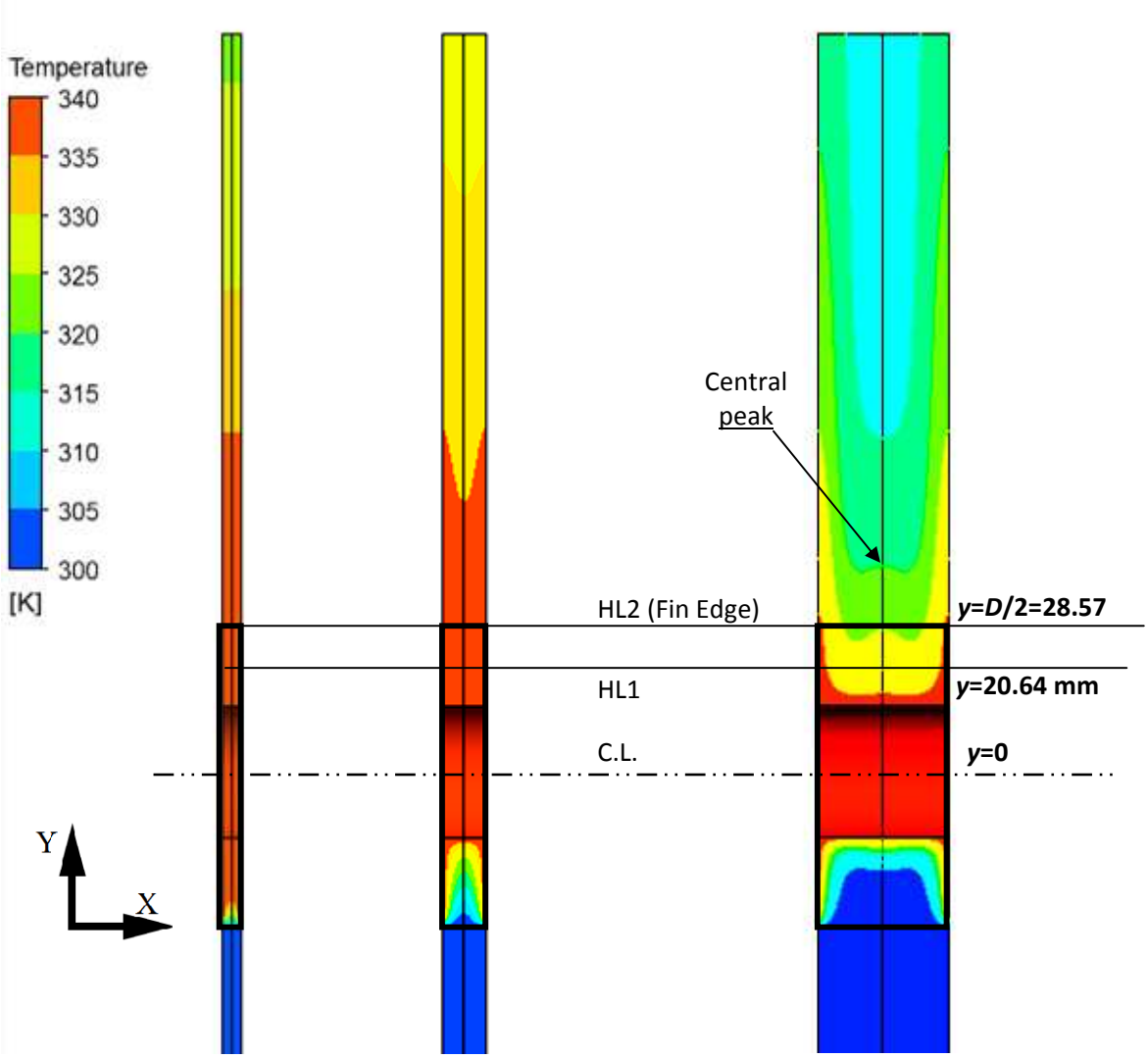

Fin number=276 Fin number=118 Fin number=39

Fig. 6. Temperature contours between two adjacent fins plotted in the symmetry plane at z=0 (Fig. 1a), results mirrored around the symmetry plane at x=c/2 (Fig. 1b).

(note that the lower part of the domain is not shown in full)

d= 25.4 mm, D=57.15 mm, $\Delta T = 40$ °C

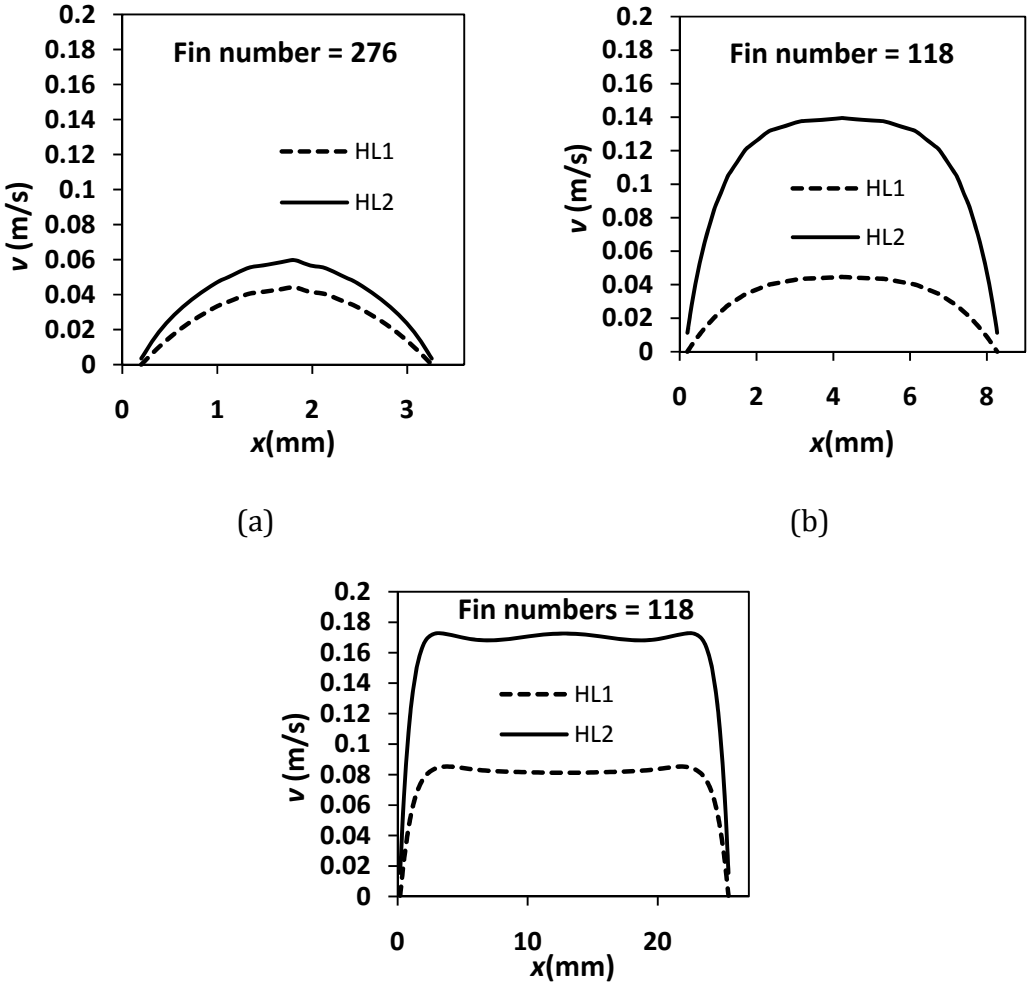

(a) (b)

(c)

Fig. 7. Air velocity profiles between two fins.

d= 25.4 mm, D=57.15 mm, $\Delta T = 40$ ℃

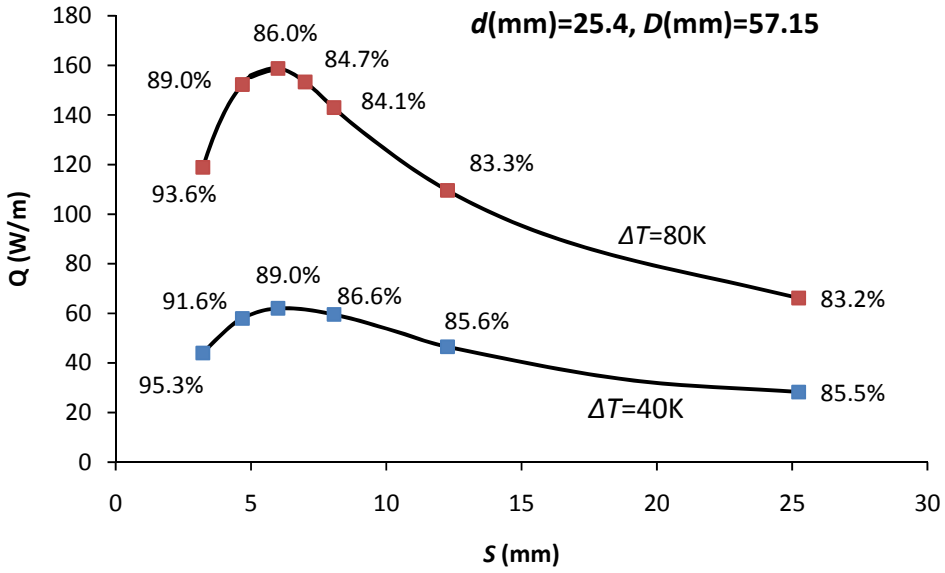

Fig. 8. Heat transfer rate from one metre of finned tube for various fin spacings based on CFD results.

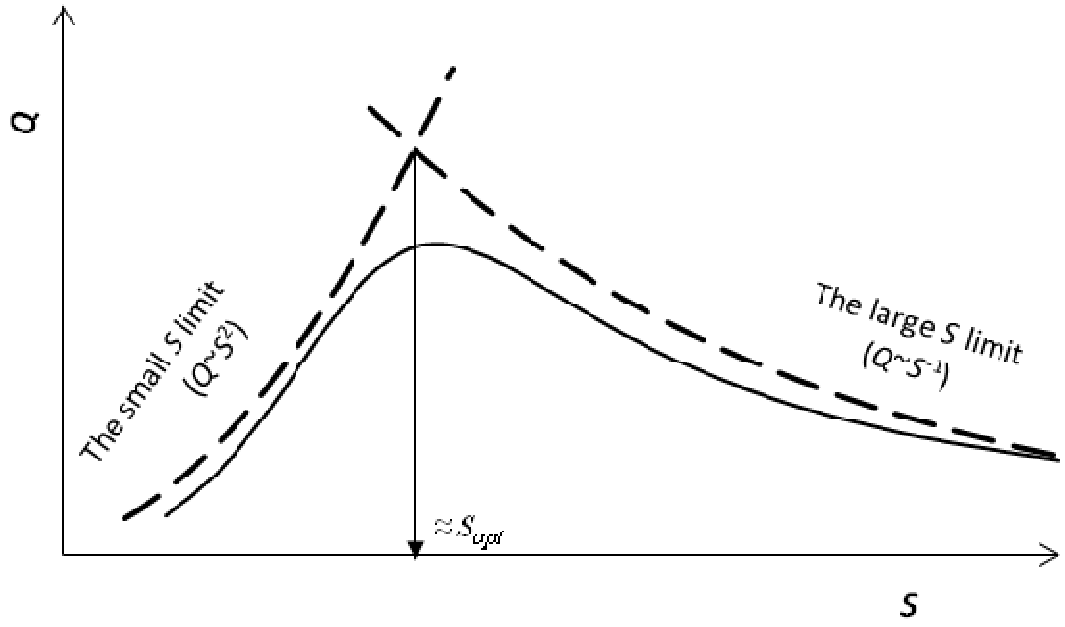

Fig. 9. Asymptotic plot for extreme limits

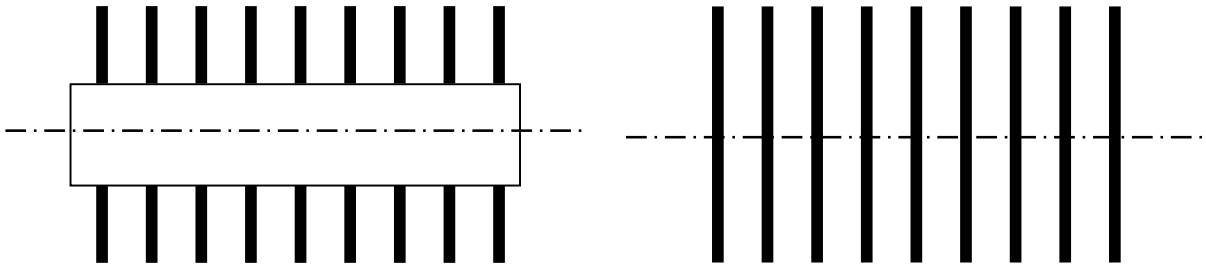

(a) (b)

Fig. 10. The limiting case, d=0 for annular fin (a) is similar to parallel circular disks (b)

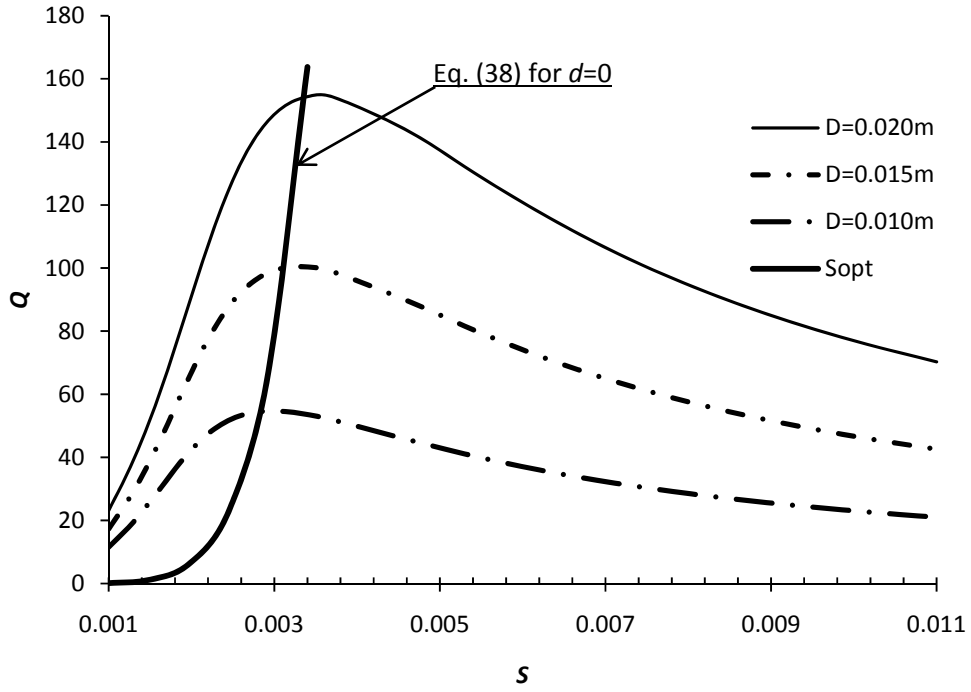

Fig. 11. Variation of convection heat transfer rate for parallel circular disks with fin spacing at different disk diameters

Notes on contributors

Hossain Nemati is an associate professor of mechanical engineering at Marvdasht University, Iran. He received his Ph.D. from Shiraz University, Iran, in 2011. His research includes free convection heat transfer, solar energy, and finned tube, as well as heat transfer optimization. He is the author or co-author of more than 40 papers in top peer-reviewed journals and a book entitled "Fundamentals of Heat Exchangers; Selection, Design, Construction and Operation". He also has gained more than 20 years of industrial experience in thermal and mechanical designs of different equipment in Oil, Gas and Petrochemical plants.

Mohammad Moghimi Ardekani is an Associate Professor of Clean Energy Technologies in Staffordshire University (UK). He has several years of academic and industrial experiences and been actively involved in the design and optimisation of new technologies and devices in the fields of renewable energy (solar thermal technologies in particular), thermal energy storage, and multiphase-based (including nanofluid) heat sinks. He has published 55 articles in top peer-reviewed journals and prestigious conference proceedings, one book, two book chapters and a webinar. His research findings gained him several international awards including Green Talents from German Ministry of education and Research. He is a charted Engineer and fellow or member of various professional institutes and societies such as Institution of Mechanical Engineering and Higher Education Academy. He is in the editorial board and reviewer of 3 and 19 notable accredited journals, respectively.

Ali Cemal Benim received his BSc and MSc in Mechanical Engineering from the Bosphorus University of Istanbul, Turkey, and PhD degree from the University of Stuttgart, Germany in 1988. Following his Postdoctoral period at the University of Stuttgart, he joined ABB Turbo Systems Ltd. in Baden, Switzerland in 1990. He was the Manager of the Computational Flow and Combustion Modelling group. Since 1996, he is Professor for Flow Simulation and Energy Technology at the Düsseldorf University of Applied Sciences, Germany.

Josua Meyer is a professor and Head of the Department of Mechanical and Aeronautical Engineering at the University of Pretoria, South Africa. He specializes in heat transfer, fluid mechanics and thermodynamic aspects of heating, ventilation and air-conditioning. He is the author and co-author of more than 800 articles, conference papers and patents, and has received various prestigious awards for his research. He is also a fellow or member of various professional institutes and societies and is regularly invited as keynote speaker at international conferences. He is the recipient of various teaching awards. He is on the editorial board and/or (lead) editor of 15 journals (including an associate editor of *Heat Transfer Engineering*), and was a member of the scientific committees of more than 40 international conferences, and conference chair of more than 15 international conferences.